Molecular dynamics study of temperature-dependent ripples in monolayer and bilayer graphene on 6H–SiC surfaces*

Tang Chao(唐 超)†, Wei Xiao-Lin(魏晓林), Tan Xin(谭 歆), Peng Xiang-Yang(彭向阳), Sun Li-Zhong(孙立忠), and Zhong Jian-Xin(钟建新)

Department of Physics & Key Laboratory for Quantum Engineering and Micro-Nano Energy Technology, Xiangtan University, Xiangtan 411105*, China*

(Received 22 June 2011; revised manuscript received 8 November 2011)

Using classical molecular dynamics and a simulated annealing technique, we show that microscopic corrugations occur in monolayer and bilayer graphene on 6H–SiC substrates. From an analysis of the atomic configurations, two types of microscopic corrugations are identified, namely periodic ripples at room temperature and random ripples at high temperature. Two different kinds of ripple morphologies, each with a periodic structure, occur in the monolayer graphene due to the existence of a coincidence lattice between graphene and the SiC terminated surface (Si- or C-terminated surface). The effect of temperature on microscopic ripple morphology is shown through analysing the roughness of the graphene. A temperature-dependent multiple bonding conjugation is also shown by the broad distribution of the carbon–carbon bond length and the bond angle in the rippled graphene on the SiC surface. These results provide atomic-level information about the rippled graphene layers on the two polar faces of the 6H–SiC substrate, which is useful not only for a better understanding of the stability and structural properties of graphene, but also for the study of the electronic properties of graphene-based devices.

Keywords: ripples, graphene, molecular dynamics

PACS: 68.65.Pq, 68.55.J–, 71.15.Pd **DOI:** 10.1088/1674-1056/21/6/066803

1. Introduction

Graphene, an isolated plane of carbon atoms arranged on a honeycomb lattice, is becoming a new star of condensed matter physics, because of its outstanding electronic properties and a high potential for applications.[1−3] In particular, the recent developments of graphene are attracting great attention as a new and unique electronic material[4−7] owing to its room-temperature quantum Hall effect,[8] together with large coherence length and high electronic mobility.[9]

Graphene is the latest carbon allotrope discovered experimentally. From the point of view of an ideally perfect crystal, graphene has a strictly two-dimensional (2D) carbon structure, in which the unit cell contains two equivalent carbon atoms (named A and B). Because of this peculiar lattice, graphene electrons behave like relativistic, massless fermions, together with near-ballistic transport at room temperature and high carrier mobility.[3−6] Recently, it has been claimed that a free-standing isolated graphene layer is intrinsically corrugated at a microscopic atomic level, i.e., the suspended graphene sheets are not perfectly flat but exhibit microscopic ripples or roughness so that the surface normally varies by several degrees and the out-of-plane deformation can reach 1 nm.[10−13] Since graphene sheets must be supported on a substrate for fabrication and applications, the effect of the substrates on the morphology of monolayer or multilayer graphene requires further investigation. Recently, a periodic ripple has been found in graphene sheets placed on various metal substrates, such as Ru (001), Ir (111), and Cu (111).[14−17] The formation mechanism of these ripples differs from that for the free-standing graphene, in which the roughening of the carbon plane is related to the instability of a perfect two-dimensional crystal. Furthermore, the experimental results supported by scanning tunneling microscopy (STM),[18] Raman spectra,[19] atomic

*Project supported by the National Natural Science Foundation of China (Grant Nos. 11047135 and 10874143), the Program for New Century Excellent Talents in University (Grant No. NCET-10-0169), and the Research Foundation of Xiangtan University, China (Grant Nos. 09QDZ08 and 10XZX04).

†Corresponding author. E-mail: tang_chao@xtu.edu.cn

© 2012 Chinese Physical Society and IOP Publishing Ltd

force microscopy (AFM),[20] and angle-resolved photoelectron spectroscopy (ARPES),[21] have revealed that the morphology of graphene is influenced by the interaction between graphitic layers and the underlying substrate. These ripples have strong effects on the electronic structure and the transport properties of graphene.

A single-atomic-layer graphene sheet was firstly produced using a micromechanical cleaving technique,[3,22] while the most promising approach to obtain graphene with an area exceeding thousands of square microns for practical electronic applications is "epitaxial" growth on SiC surfaces.[4,5] Namely, graphene layers can be produced by sublimating Si atoms from either the 4H– or 6H–SiC surfaces at sufficiently high temperatures to graphitize the excess carbon. Recent theoretical and experimental results have demonstrated that the electronic property of graphene layers on SiC substrates differs from that of isolated graphene because of the existence of a strong covalent bond between the substrate and the graphene layers.[23,24] Extensive *ab initio* calculations supported by the STM experiments also show clear evidence of a strong nanostructuration of the interface carbon layer between graphene and an Si-terminated SiC surface.[25] So, it is interesting to investigate the atomic morphologies and the electronic properties of graphene on the different substrates. On the other hand, obtaining the stable configurations of graphene layers, studying their electronic properties, and understanding their fundamental physics are essential steps toward device realization. Controlling the surface or interface morphology of graphene layers on the two polar hexagonal SiC surfaces should be a priority for future applications. For instance, how the SiC substrate affects the specific structure of graphene, and what the details about the interface between graphene and the substrate are. Consequently, an atomic-level understanding of the nanoscale structures of monolayer and multilayer graphene on SiC substrates is crucial to explaining the observed electronic structure and transport properties.

In the present paper, we perform a classical molecular dynamics (MD) study of the ripples in monolayer (MLG) and bilayer (BLG) graphene on the two polar 6H–SiC surfaces (Si-terminated surface and C-terminated surface). We use simulated annealing to obtain the minimal energy configurations of the MLG and the BLG on 6H–SiC substrates and investigate the microscopic roughness of the ripples through analysing the bonding conjugations of carbon atoms in graphene layers, associated with the change in temperature.

2. Model and computational method

Our calculations are performed using the MD and the simulated annealing technique. The semi-empirical many-body Tersoff potential is employed to describe the C–C, Si–Si, and Si–C interactions in the simulation.[26] The constant number of particles-volume-temperature (NVT) ensemble is used for the simulation environment. The Newton equation of motion is solved by the fifth-order Gear algorithm, with a time step of $\Delta t = 1$ fs. The temperature is controlled by the velocity scaling method, and the cut-off distance for interatomic interaction is chosen to be 10 Å (1 Å=0.1 nm) for all atoms. A standard simulated annealing process is used to find the stable configuration of graphene on the 6H–SiC surface, and this has been widely used in recent years to computationally search for the lowest-energy structures of the nanostructures.[27−29]

In our simulations, the simulated 6H–SiC substrate consists of 12 planes (six pairs of C and Si planes) with $N = 4608$ in a 73.9×49.3×47.9 Å rhombic cell. Two sets of calculations (with monolayer and bilayer graphene on SiC substrates) were performed on both the Si- and C-terminated surfaces. To start, the graphene monolayer is made up of carbon atoms on a flat and complete honeycomb lattice. The distance between the graphene and the SiC surfaces is set to be approximately 2 Å. The second set of calculations includes the BLG on top of the SiC substrate. In the BLG, the two carbon layers are arranged with the atoms in one layer located on the top of the centre of a hexagon in the other layer, i.e., AB stack. In both calculation sets, the periodic boundary conditions along the x and the y directions are taken into account so that both the graphene layers and substrate can be viewed as infinitely large in these dimensions. In order to maintain a reasonable computation time, we keep the atoms in the lowest SiC bilayer fixed at a bulk position. A simulated annealing process is performed to find the stable morphology of the graphene layer on the SiC substrate. In this process, the configuration of graphene is relaxed for $\Delta t = 100$ ps at each simulated temperature, and then reaches a local minimum energy configuration by means of the simulated annealing, with a cooling rate of $R = 10$ K/ps. Using the MD simulation, the roughness morphologies of MLG and BLG on SiC substrates are displayed. The effect of temperature on the ripple is also studied through analysing the covalent bonding inhomogeneities in the

bond-length and bond-angle distributions. The MD simulation results are illustrated in Figs. 1–7.

3. Results and discussion

Figure 1 shows the atomic configurations of MLG and BLG on Si-terminated 6H–SiC (0001) surfaces, associated with the change in temperatures. For the MLG on the Si-terminated surface, one can easily identify two different kinds of microscopic corrugation structures, namely periodic ripples and random ripples. At room temperature (T = 300 K), an atomic configuration with periodic corrugations is very clear in MLG on the Si-terminated SiC (0001) surface (see Fig. 1(a)). An elaborate atomic pattern of MLG on the Si-terminated 6H–SiC (0001) surface is also shown in Fig. 2, in which a periodic rippled structure with a triangle is very apparent. The wavelength of the ripples presents a periodicity of 12.3±0.1 Å, and the height is about 1.4 Å (see Fig. 2(d)). These periodic ripples should come from the coincidence lattice of the graphene and Si-terminated surface, differing from the roughening of the free-standing monolayer graphene due to the instability of a strictly two-dimensional crystal. It can be found that the lattice of graphene has a size relation to the underlying Si lattice of the Si-terminated SiC surface, namely, five carbon honeycombs (0.246 nm) will be adjusted almost exactly with four Si–Si interatomic distances (0.308 nm) on the Si-terminated surface of 6H–SiC (0001). This slight lattice mismatch between SiC and graphene results in a structural strain at low temperature. Thus, the graphene layer is rippled in a periodic fashion, with a periodicity determined by the difference between the lattice parameters. However, high temperature affects the lattice mismatch between MLG and the substrate due to a difference in the thermal expansion coefficient between graphene and SiC. At high temperature, a larger and random corrugation occurs in the MLG as shown in Figs. 1(b)–1(e). Nevertheless, the amplitudes of these ripples are much smaller than those found in free-standing monolayer graphene. The maximal height of the random ripple in MLG on the SiC surface is around 1.6 Å and the wavelength reaches ∼ 18 Å.

We further investigate the temperature-dependence of the ripples in BLG on the Si-terminated 6H–SiC (0001) surface. In our simulation, the BLG consists of two layers of graphene sheets with AB stacking, namely the bottom and top graphene layers. In Figs. 1(f)–1(j), the atomic configurations of the top layer of the BLG are shown at temperatures ranging from 300 K to 2500 K. One can see that the top layer is almost flat at room temperature and random ripples appear at high temperature. At room temperature, a detailed atomic configuration of BLG on the Si-terminated SiC substrate is shown in Fig. 3. In the BLG, a slight ripple still occurs in the top graphene layer (see Fig. 3(a)), and the ripples have an amplitude of 0.04 nm for a wavelength of 1.2 nm. The periodic ripples are also displayed in the bottom graphene layer as shown in Fig. 3(b). One can find that the top layer of BLG tends to follow the morphology of the bottom layer so that the amplitude modulation of ripples in the top layer is smaller than that of the bottom layer (see Figs. 3(c) and 3(d)). Nevertheless, the corrugation of the bottom graphene layer of BLG is still clear, in which a height difference between the lower atom and the upper atom is close to 0.07 nm. This height is only half the one found in MLG.

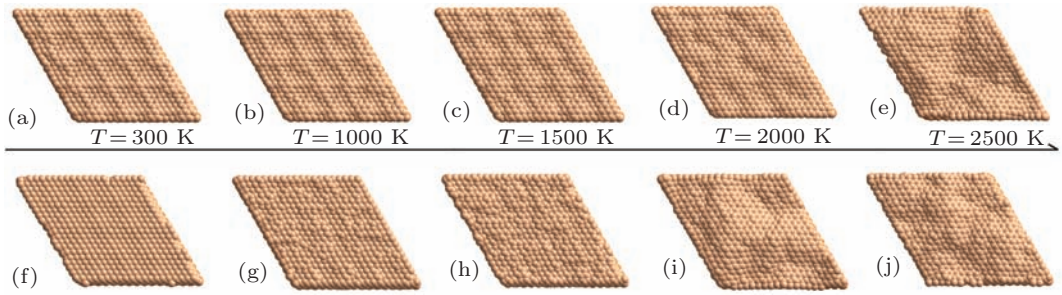


Fig. 1. (colour online) Top view of the rippled configurations of the MLG and the BLG on the top of the Si-terminated 6H–SiC surface associated with a change in temperature. Panels (a)–(e) show the atomic configurations of the ripples in MLG at temperatures ranging from 300 K to 2500 K, and panels (f)–(j) exhibit the atomic configurations of the ripples in the BLG.

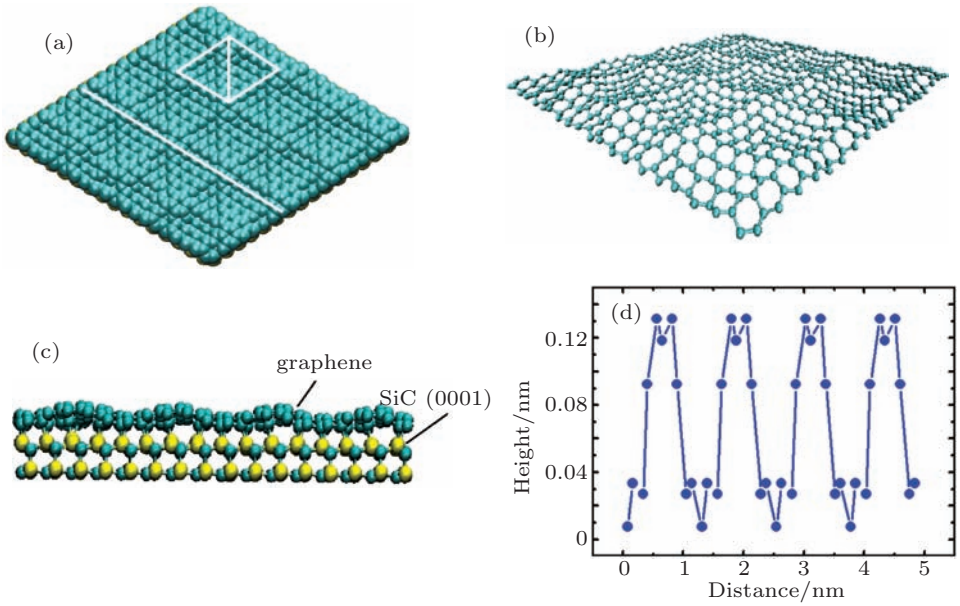


Fig. 2. (colour online) (a) The periodic corrugation of MLG on an Si-terminated SiC surface at room temperature ($T = 300$ K). (b) A three-dimensional (3D) schematic illustration of the rippled MLG in panel (a). (c) Cross section of the MLG with periodic atomic corrugations. (d) A height profile of the carbon atoms along the line defined in panel (a). The atomic corrugation in MLG is around 0.14 nm at room temperature.

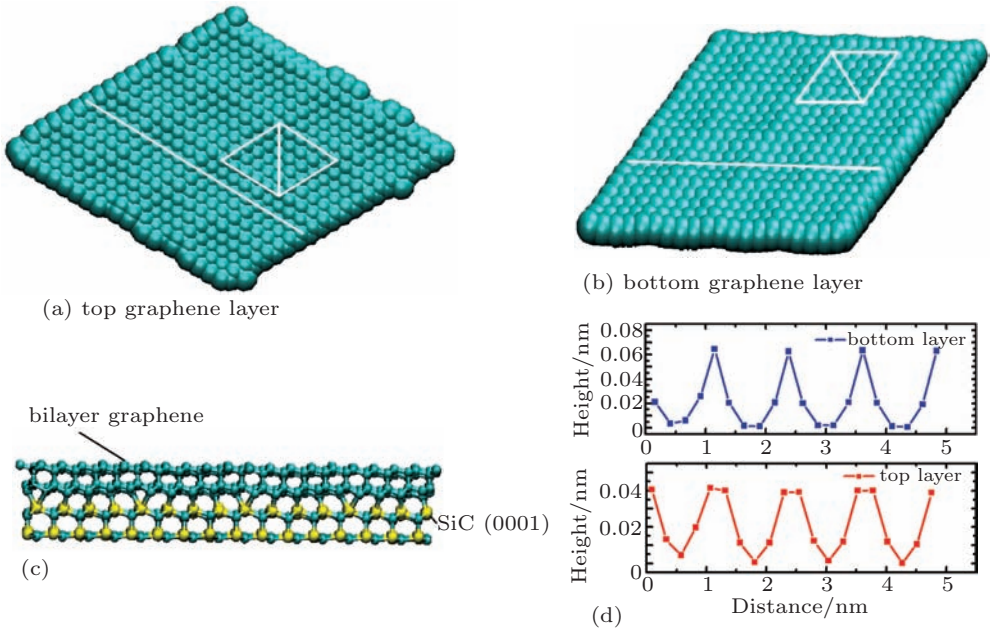


Fig. 3. (colour online) Atomic configurations of BLG on an Si-terminated SiC surface at room temperature. (a) The top graphene layer of BLG. (b) The bottom graphene layer of BLG. (c) Cross section of BLG with periodic atomic corrugation. (d) Height profiles of the top and bottom layer atoms along the lines marked, respectively, in panels (a) and (b).

In order to show the microscopic fluctuations of the carbon atoms of graphene on the SiC substrate, the surface roughness, $R_{\rm a}$, of the rippled graphene is evaluated from[30]

$$R_{\rm a} = \sum \frac{|Z_i - Z_{\rm ave}|}{N}, \tag{1}$$

where N is the number of measured heights in the rippled graphene on the SiC substrate, Z_i is the height of the surface carbon atoms, and $Z_{\rm ave}$ is the average height of all the carbon atoms within the rippled graphene. We investigate the effect of temperature on the microscopic roughness of graphene layers on

the Si-terminated SiC surface. As shown in Fig. 4(a), the temperature dependences of the roughness of rippled MLG and BLG are displayed. For the MLG, a clear enhancement in the roughness is displayed as the temperature increases. For the BLG, we have calculated the roughnesses of the bottom and top graphene layers, and compared them with that of the MLG. We find that at low temperature ($T \leq 1500$ K), the roughness of the top layer of BLG is much smaller than that of MLG. However, at high temperature ($T > 1500$ K), the top layer shows larger microscopic roughness, close to that of MLG. In contrast to the top layer of BLG, the enhancement of the roughness of the bottom layer is slower, and is associated with an increase in temperature. At low temperature, the corrugation of the bottom layer is larger than that of the top layer, but smaller than the one found in MLG. Therefore, the bottom graphene layer can be regarded as a buffer layer between the SiC substrate and the top layer of the BLG. The buffer layer smoothes down the ripples of the top graphene layer, so that the BLG seems to be flatter than the MLG.

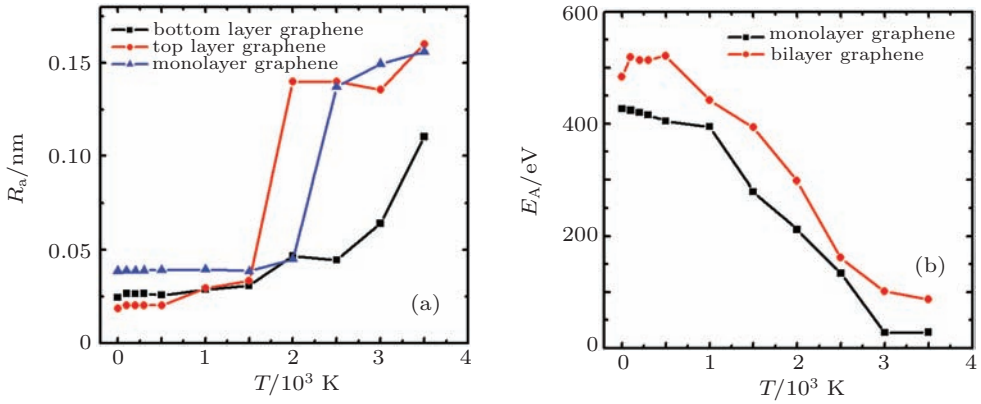


Fig. 4. (colour online) (a) The surface roughnesses of the MLG, the top graphene layer and the bottom graphene layer on the Si-terminated SiC surface, each as a function of temperature. (b) The adhesive energies of the MLG and the BLG on the top of the Si-terminated SiC surface, each as a function of temperature.

In addition, we have studied the adhesive energies of the MLG and the BLG. The adhesive energy E_A can be defined as $E_A = N^{-1}(E_{Sub} + E_{GNR} - E)$, where E_{Sub} is the total energy of the SiC substrate, E_{GNR} is the total energy of the freestanding graphene, E is the energy of the whole system including graphene and the substrate, and N is the number of all the carbon atoms in graphene. All the calculations have been performed in the same simulation cell. The temperature dependence of the adhesive energy E_A is shown in Fig. 4(b). The values of E_A for both MLG and BLG on the Si-terminated SiC surface decrease, which is associated with the increase in temperature. This suggests that the falling strength of the interaction between the graphene layer and SiC substrate is accompanied by a gradual change in graphene morphology from an almost flat surface to a strongly corrugated surface. In Fig. 4(b), we find that the adhesive energy of BLG is stronger than that of MLG, which suggests that a stronger adhesive behaviour occurs between BLG and the substrate, so that the BLG ripples are smaller than those of MLG.

We also investigate the atomic configurations of MLG on the C-terminated SiC surface to compare them with the Si-terminated surface. The simulation cells used for the calculations are equivalent. As shown in Fig. 5, the periodic ripples also occur in the MLG placing on a C-terminated SiC surface at room temperature, and show a hexagon of gibbose shape, namely, a honeycomb pattern with a size of 12.3×12.3 Å (see Fig. 6(a)), which is different from the periodic ripples with a cupped-shape triangle in the MLG on the Si-terminated SiC surface. In addition, the temperature dependences of the microscopic roughness and the adhesive energy of the MLG on Si- and C-terminated surfaces have been studied. As shown in Fig. 6(c), an enhancement in the roughness of the MLG occurs, which is associated with the increase in temperature. We find that the roughness is smaller on the C-terminated surface than on the Si-terminated surface at low or high temperature. The MD simulation results are in good agreement with the experimental results, in which the graphene layer seems to be flatter on the C-terminated SiC surface than on the Si-terminated SiC surface, since the bonding strengths of the graphene layer to the substrate are different.[23] The adhesive energy of MLG on the C-terminated surface is also smaller than that on the Si-

terminated surface at low temperature (see Fig. 6(d)). In the C-terminated case, the MD simulations show that only a few covalent C–C bonds are formed in the interface between MLG and the substrate (see Fig. 6(b)). Although C–C bonds are stronger and shorter than Si–C bonds, the number of C–C bonds is so small that the adhesive energy of MLG on the C-terminated SiC surface is not high. The molecular dynamics results reveal that the microscopic ripples induced by the coincidence lattice between the graphene and substrate affect the strength of the substrate-graphene bonding.

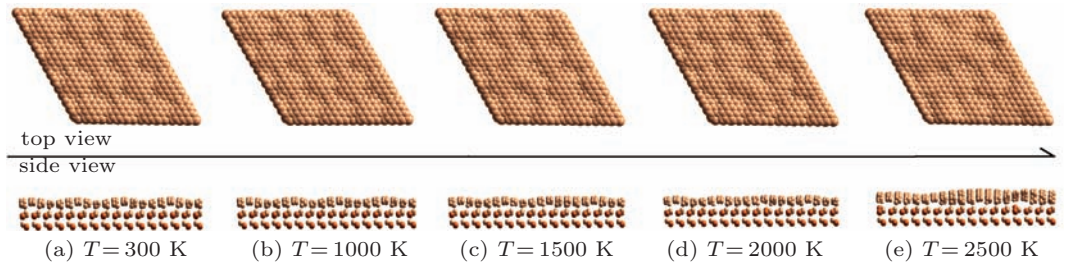


Fig. 5. (colour online) Top and side views of the rippled atomic configurations of the MLG on the top of the C-terminated SiC surface associated with the change in temperature.

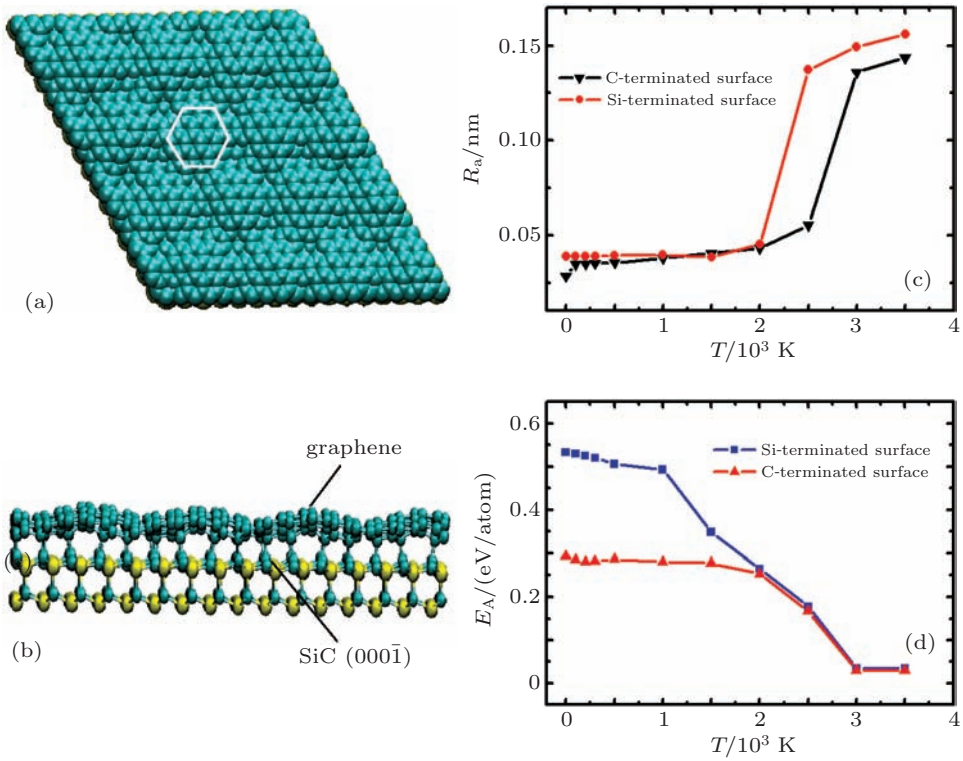


Fig. 6. (colour online) (a) Top view of the atomic configuration of the MLG on the C-terminated SiC surface at room temperature. (b) Cross section of the MLG with periodic atomic corrugation. (c) Surface roughnesses of the MLG on the Si-terminated and the C-terminated SiC surfaces, each as a function of temperature. (d) Temperature dependences of the adhesive energy of MLG on the Si- and C-terminated SiC surfaces.

The temperature dependence of the microscopic roughness of the ripples on two polar faces of the 6H–SiC substrate is also studied through analysing the covalent bonding inhomogeneities in bond-length and bond-angle distributions. We calculate the pair correlation functions (PCFs) and the bond-angle distributions of rippled MLG on C- and Si-terminated SiC surfaces. The pair correlation function $g_{ij}(r)$ indicates the average number of atoms (of atomic species i) per unit volume of atomic species j atoms that are located at distance r from a target atomic species i atom. The number is expressed in terms of average density N_j/V.

The pair correlation function $g_{ij}(r)$ is defined as follows:

$$g_{ij}(r) = \frac{V}{N_i - N_j} \sum_{k}^{N_i} \frac{n_{kj}(r - \Delta r/2, r + \Delta r/2}{4\pi r^2 \Delta r}, \quad (2)$$

where N_i is the total number of atomic species i atoms included in the system, and n_{ik} is the number of atomic species k atoms included in a spherical shell of thickness Δr located at a distance r. For atoms of the same species, $N_j = N_i - 1$. The PCFs and the bond-angle distributions for different temperatures are shown in Fig. 7, which shows the changes in the bond conjugation of the rippled MLG. We can find from Figs. 7(a) and 7(c) that at room temperature, all the first neighbour bonds of the carbon atoms in MLG on the C- or Si-terminated SiC surfaces are equivalent, and very close to the interatomic distance of 1.42 Å of perfect graphene, while a broad distribution of the first neighbour bond lengths is shown at high temperature, giving longer bonds of carbon (1.52 Å). This indicates that there is a large probability of having a broad distribution of short/long bonds, which is associated with local deviation from planarity. Similarly, the ripples of MLG produce a broader distribution of carbon–carbon bond angles and induce various bonding conjugations as the temperature changes. In Fig. 7(b), the angular distribution at 300 K shows two peaks, one around 120°, and the other 109°. This could indicate the formation of an sp^3 state of carbon in rippled graphene. Similar results occur in the case of the C-terminated 6H–SiC surface as shown in Fig. 7(d). Our MD results suggest that extrinsic ripples in graphene can produce structural distortions, showing domains with lower than hexagonal symmetry. Such domains can exhibit an admixture of sp^2 and sp^3 carbon orbital character and π orbital misalignment. Thus, it is believed that MLG placing on a C- or Si-terminated 6H–SiC surface has a tendency to form inhomogeneous bond patterns associated with the microscopic fluctuations of carbon atoms at different temperatures.

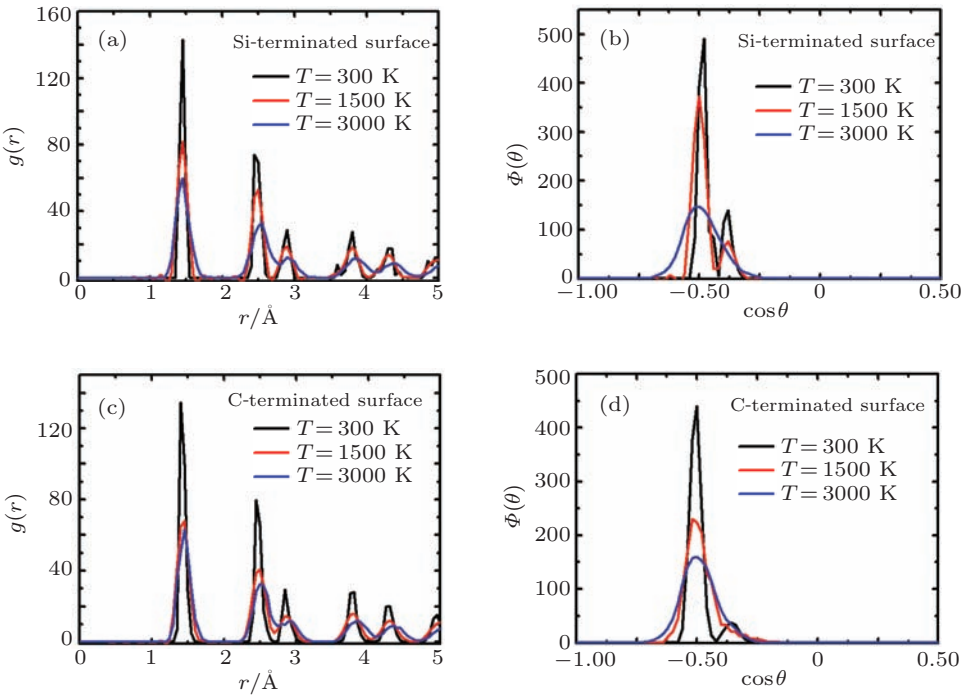


Fig. 7. (colour online) (a) The pair correlation functions of the rippled MLG on the Si-terminated SiC surface at $T = 300$ K, $T = 1500$ K, and $T = 3000$ K. (b) Variations in the carbon–carbon bond angle distributions of the rippled MLG (a) at different temperatures. (c) Pair correlation functions of the rippled MLG on the C-terminated SiC surface at different temperatures. (d) Carbon–carbon bond angle distributions of the rippled MLG in panel (c).

4. Conclusions

Using classical molecular dynamics, we show that microscopic ripples occur in both MLG and BLG coverings on the top of Si- or C-terminated 6H–SiC substrates. Our atomic scale simulations indicate that two types of microscopic corrugations are present in both MLG and BLG associated with the change in temperature, namely the periodic ripples at room temperature and the random ripples at high temperature.

We also show the rippled morphologies of the MLG on Si-terminated and C-terminated SiC surfaces through analysing the atomic configurations and the microscopic roughnesses. We find that the periodic corrugation of the MLG on an Si-terminated SiC surface is different from that on a C-terminated SiC surface. The former shows a cupped-shaped triangle, and the latter a hexagon of gibbose shape. In addition, the inhomogeneity of carbon covalent bonding in the rippled graphene is identified through analysing the bond-length and the bond-angle distribution. A broad distribution of the carbon–carbon bond lengths and the bond angles are shown when the temperature increases, which implies that a temperature-dependent multiple bonding conjugation occurs in the graphene sheet on the SiC surface. These results provide atomic-level information about the rippled graphene layers on the SiC substrate, which are useful not only for a better understanding of the stability and structural properties of graphene, but also for the study of the electronic transport properties of graphene-based devices.

References

[1] Novoselov K S, Geim A K, Morozov S V, Jiang D, Katsnelson M I, Grigorieva I V, Dubonos S V and Firsov A A 2005 *Nature* **438** 197

[2] Zhang Y, Tan Y W, Stormer H L and Kim P 2005 *Nature* **438** 200

[3] Novoselov K S, Jiang D, Schedin F, Booth T J, Khotkevich V V, Morozov S V and Geim A K 2005 *Proc. Natl. Acad. Sci. USA* **102** 10451

[4] Berger C, Song Z, Li X, Wu X, Brown N, Naud C, Mayou D, Li T, Hass J, Marchenkov A N, Conrad E H, First P N and de Heer W A 2006 *Science* **312** 1191

[5] Berger C, Song Z, Li T, Li X, Ogbazghi A Y, Feng R, Dai Z, Marchenkov A N, Conrad E H, First P N and de Heer W A 2004 *J. Phys. Chem.* B **108** 19912

[6] Geim A K and Novoselov K S 2007 *Nat. Mater.* **6** 183

[7] Neto A H C, Guinea F, Peres N M R, Novoselov K S and Geim A K 2009 *Rev. Mod. Phys.* **81** 109

[8] Nomura K and MacDonald A H 2006 *Phys. Rev. Lett.* **96** 256602

[9] Wu J H, Wojciech P and Klaus M 2007 *Chem. Rev.* **107** 718

[10] Mermin N D 1968 *Phys. Rev.* **176** 250

[11] Meyer J C, Geim A K, Katsnelson M I, Novoselov K S, Booth T J and Roth S 2007 *Nature* **446** 60

[12] Fasolino A, Los J H and Katsnelson M I 2007 *Nat. Mater.* **6** 858

[13] Han T W and He P F 2010 *Acta Phys. Sin.* **59** 3408 (in Chinese)

[14] Marchini S, Günther S and Wintterlin J 2007 *Phys. Rev.* B **76** 075429

[15] Pan Y, Shi D X and Gao H J 2007 *Chin. Phys.* **16** 3151

[16] N'Diaye A T, Coraux J, Plasa T N, Busse C and Michely T 2008 *New. J. Phys.* **10** 043033

[17] Gao L, Guest J R and Guisinger N P 2010 *Nano Lett.* **10** 3512

[18] Xu K, Cao P and Heath J R 2009 *Nano Lett.* **9** 4446

[19] Dong S L, Christian R, Benjamin K, Klaus K, Ulrich S and Jurgen H S 2008 *Nano Lett.* **8** 4320

[20] Ishigami M, Chen J H, Cullen W G, Fuhre M S and Williams E D 2007 *Nano Lett.* **7** 1643

[21] Ohta T, Bostwick A, McChesney J L, Seyller T, Horn K and Rotenberg E 2007 *Phys. Rev. Lett.* **98** 206802

[22] Novoselov K S, Geim A K, Morozov S V, Jiang D, Zhang Y, Dubonos S V, Grigorieva I V and Firsov A A 2004 *Science* **306** 666

[23] Varchon F, Feng R, Hass J, Li X, Nguyen B N, Naud C, Mallet P, Veuillen J Y, Berger C, Conrad E H and Magaud L 2007 *Phys. Rev. Lett.* **99** 126805

[24] Mattausch A and Pankratov O 2007 *Phys. Rev. Lett.* **99** 076802

[25] Varchon F, Mallet P, Veuillen J Y and Magaud L 2008 *Phys. Rev.* B **77** 235412

[26] Tersoff J 1989 *Phys. Rev.* B **39** 5566

[27] Ivashchenko V I, Turchi P E A, Shevchenko V I and Shramko O A 2004 *Phys. Rev.* B **70** 115201

[28] Zhang K W, Stocks G M and Zhong J X 2007 *Nanotechnology* **18** 285703

[29] Meng L J, Zhang K W, Stocks G M and Zhong J X 2007 *J. Appl. Phys.* **100** 126107

[30] Haerle R, Baldereschi A and Galli G 2000 *J. Non-Cryst Solids* **740** 266